

# METAMORPHOSIS OF AN ENZYME

Rudolf Ladenstein, Winfried Meining, Xiaofeng Zhang,  
Markus Fischer & Adelbert Bacher

The protein shells of the bifunctional Lumazine/Riboflavin synthase complex found in bacteria, archaea and plants show some similarity to the assembly of small spherical viruses. Sixty lumazine synthase subunits form a  $T = 1$  icosahedral capsid, which instead of nucleic acids in the central core, contains a trimer of riboflavin synthase. Lumazine synthases from fungi, yeasts and some bacteria, however, exist only in pentameric form. Capsid formation in icosahedral lumazine synthases is dependent on the presence of certain substrate-analogous ligands, on pH and phosphate concentration. The experimental background from X-ray crystallography, X-ray small angle scattering and electron microscopy will be discussed. Different active assemblies of the enzyme are observed *in vivo* and *in vitro*. There is experimental evidence for the formation of large capsids, obtained spontaneously or after certain mutations to the sequence of the lumazine synthase subunit. Those presumably metastable  $T = 3$  capsids can be reassembled into  $T = 1$  capsids by ligand-driven reassembly *in vitro*. The active site of lumazine synthase is relatively resilient to point mutations. One lethal mutation to the binding site for the phosphate-substrate, however, has a strong influence on both, capsid stability and enzymatic activity.

*Keywords:* lumazine synthase, riboflavin synthase, protein dissociation and association, vitamin biosynthesis, X-ray crystallography

## 1. ...1980 AT TU MUNICH...

A surprisingly large enzyme complex was isolated and purified from the cell contents of *Bacillus subtilis* in 1980 at the Technical University of Munich (Mailänder & Bacher, 1976; Bacher *et al.*, 1980a). The complex, which was initially called “heavy riboflavin synthase”, was a  $10^6$  Dalton protein (26 S) that consisted of two types of subunits, which were

designated as  $\alpha$  ( $M = 23500$  Da) and  $\beta$  ( $M = 16000$  Da). It was found that the enzyme catalysed two subsequent reactions of the riboflavin biosynthesis pathway, shown in Fig 1 (Nielsen *et al.*, 1984).

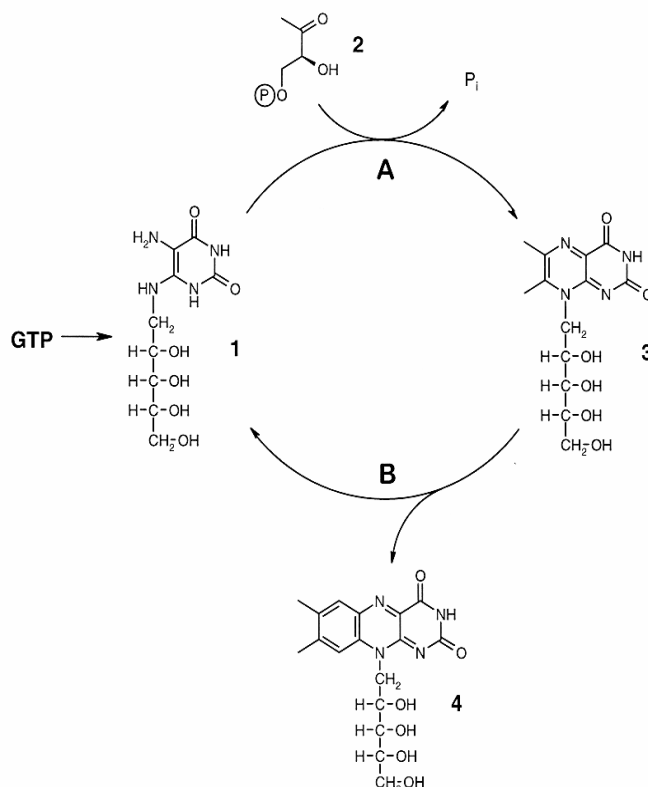


Fig 1. Reaction catalyzed by the bifunctional lumazine synthase (A) riboflavin synthase (B) complex.

At this time, the second substrate (**2**) was still unknown, but a four carbon compound was suggested (Le Van *et al.*, 1985). The molecular structure of “heavy riboflavin synthase” showed a number of unexpected features. The subunit stoichiometry was striking with 3  $\alpha$  subunits and 60  $\beta$  subunits. Electron micrographs obtained by negative staining showed approximately spherical particles with a diameter of 150 Å,

shown in Fig 2 (Bacher, 1980b). Binding experiments with antibodies raised against  $\alpha$  subunits showed that the immunological determinants of the  $\alpha$  subunits were inaccessible in the native enzyme complex (Bacher, 1986). On the basis of these preliminary results, it was suggested that the quaternary structure of the bifunctional enzyme complex is characterized as a spherical capsid of 60  $\beta$  subunits with icosahedral symmetry, which contains a trimer of  $\alpha$  subunits in the central cavity (Bacher, 1980b).

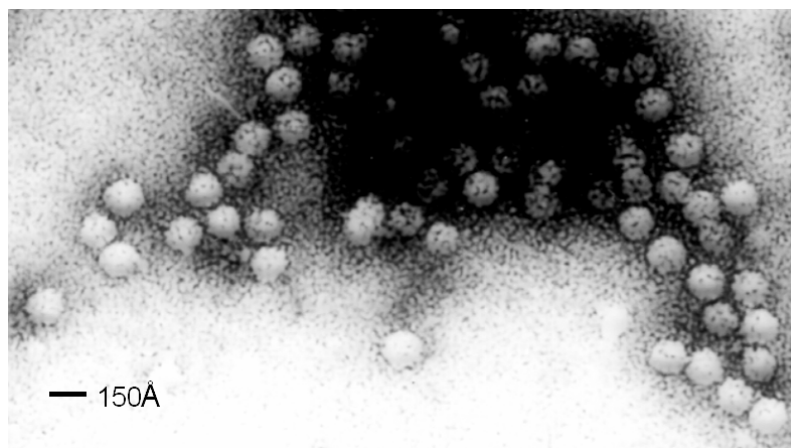


Fig 2. Negative staining electron micrograph of “Heavy Riboflavin Synthase”

With this assumption a vast field of ideas was opened, which were extremely inspiring and needed to be verified by structure-analytical techniques. At almost the same time novel and powerful crystallographic methods were developed which allowed to use the redundancy of structure information in the icosahedral tomato bushy stunt virus for phase determination (Harrison, 1978). The successful crystallization of the bifunctional enzyme complex (Ladenstein *et al.*, 1983) today designated as lumazine synthase (LS)/riboflavin synthase (RS) complex, initiated an exciting scientific adventure into structural biology, and, not less important, long-standing personal relations in between scientists from Germany, Sweden, Bulgaria, the United States and China.

## 2. DEALING WITH ICOSAHEDRAL PARTICLES

In the absence of specific ligands (substrate analogs to **1** and **3**) the enzyme complex was stable only in the presence of phosphate ions in a narrow pH range close to neutrality. Dissociation occurred in between pH 7 and 8 and led to the formation of  $\alpha$  subunit trimers. The  $\beta$  subunits reaggregated to form a polydisperse mixture of large oligomers with the shape of hollow or massive spheres and molecular weights, determined by sedimentation analysis in the analytical ultracentrifuge, of  $3 \times 10^6$  Daltons (26 S) and  $6 \times 10^6$  Daltons (48 S) (Bacher, 1980a,b).

The native and the reaggregated 26 S and 48 S particles were studied by X-ray small angle scattering on a synchrotron X-ray source (Ladenstein *et al.*, 1986 see Fig 3 for a typical scattering curve). The scattering curves of the 26S particles had a characteristic appearance and were well interpretable in terms of a hollow sphere model with a ratio of inner and outer radius of  $R_i/R_o = 0.3/1$ . For the native 26 S complex a diameter of 160 Å was estimated from the scattering curves, in good agreement with the value from electron micrographs. For the 48 S aggregate a maximum diameter of about 330 Å was observed.

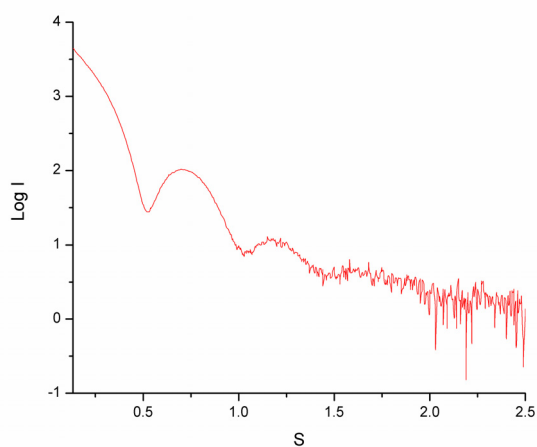


Fig 3. Typical scattering curve of the 26S (T = 1 icosahedral) particles of lumazine synthase from *B. subtilis* derived from X-ray small angle scattering.

In parallel to the initial crystallographic studies the crystals were studied by electron microscopy. Electron micrographs of freeze-etched crystals of the native complex showed approximately spherical molecules, which were arranged in hexagonal layer packing (Fig 4a, b). The lattice constants (156 Å) found from the micrographs were in excellent agreement with the values derived from X-ray diffraction data (156.4 Å). From the electron micrographs a packing model was derived which, together with the space group symmetry of the crystals (P6<sub>3</sub>22) allowed an unambiguous determination of the translation component of the particles (Ladenstein *et al.*, 1986). Silver and gold decoration patterns mapped by electron microscopy in conjunction with image processing were used to determine approximate values of the orientation of the icosahedral symmetry axes with respect to the crystal cell axes (Fig 4c) (Weinkauff *et al.*, 1991).

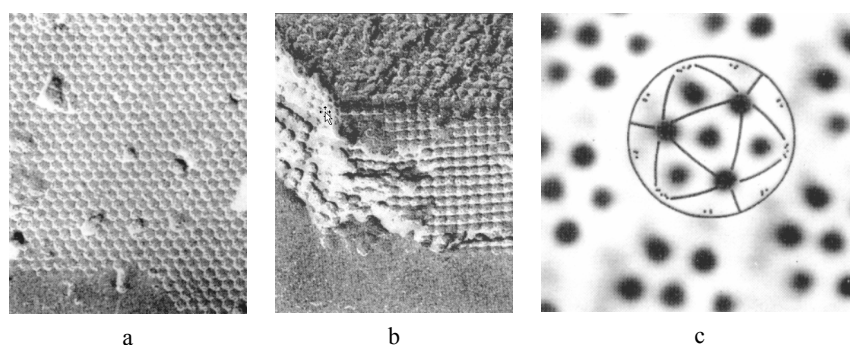


Fig 4 Electron micrographs of freeze-etched crystals of heavy riboflavin synthase. (a) ab plane; (b) ac plane; (c) silver decoration of the ab plane of a *B. subtilis* LS crystal with an overlay of an icosahedral model.

X-ray intensity data to 3.2 Å resolution were obtained at EMBL Outstation, Hamburg, Germany. Patterson self rotation functions (Rossmann & Blow, 1962) calculated from these data showed a set of peaks for two-fold, three-fold and five-fold local symmetry axes accurately consistent with icosahedral symmetry and with one of both particle orientations allowed by the crystal packing model deduced from electron microscopy. With the help of these data it was clear that the

structure of the native complex can be described as an icosahedral capsid of 60  $\beta$  subunits with the triangulation number  $T = 1$  (Ladenstein *et al.*, 1986). The spatial orientation of the  $\alpha$  subunits located in the central core, however, was incompletely understood at this time. The LS/RS complex of *Bacillus subtilis* was thus the first bifunctional enzyme with icosahedral symmetry to be investigated by X-ray crystallography.

### 3. SUBUNIT FOLD RELATED TO FLAVODOXIN

The structure of the icosahedral capsid was determined by multiple isomorphous replacement, icosahedral symmetry averaging (Bricogne, 1974; Bricogne, 1976) and phase extension to 3.3 Å resolution (Ladenstein *et al.*, 1988). Due to the limitations in computer memory and speed, phase extension in conjunction with symmetry averaging was still an enormous undertaking with respect to computing time, but was already extensively used by other colleagues in the structure analysis of spherical viruses (Rossmann *et al.*, 1985). The averaged electron density map was of high quality, but due to the static disorder of the capsids in the unit cell, contained no information on the structure of the  $\alpha$  subunits. The observed fold of the  $\beta$  subunit, a four-stranded parallel  $\beta$ -sheet flanked on both sides by pairs of  $\alpha$  helices, resembled the folding pattern of flavodoxins, although no significant sequence homology could be detected (Fig 5). The fold of the  $\beta$  subunit has no structural resemblance with the subunit structures of the known icosahedral plant or animal viruses.

The structural organization of the pentamers in the capsid is striking, due to its beauty and obvious (pH dependent!) structural stability (Karshikoff & Ladenstein, 1989) (Fig 6). The N-terminal segment of each monomer is attached to the beta sheet of the neighbouring monomer thus forming the fifth strand of the beta sheet. By helix  $\alpha_3$  and its four symmetry-related neighbours a channel is formed. The five helices are twisted into a stable super-helical motif comprising pores (diameter 9 Å, length 30 Å) in the capsid wall, which are parallel to the five-fold local symmetry axes. Due to its stability the pentamers were suggested to constitute the building blocks in the capsid assembly (Karshikoff & Ladenstein, 1989).

Experimental evidence, however, e.g. from assembly studies by X-ray or neutron scattering is still lacking.

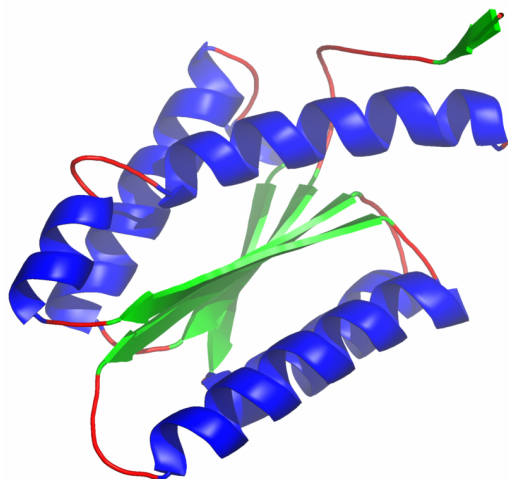


Fig. 5 Folding pattern of a  $\beta$  subunit of lumazine synthase from *B. subtilis*.

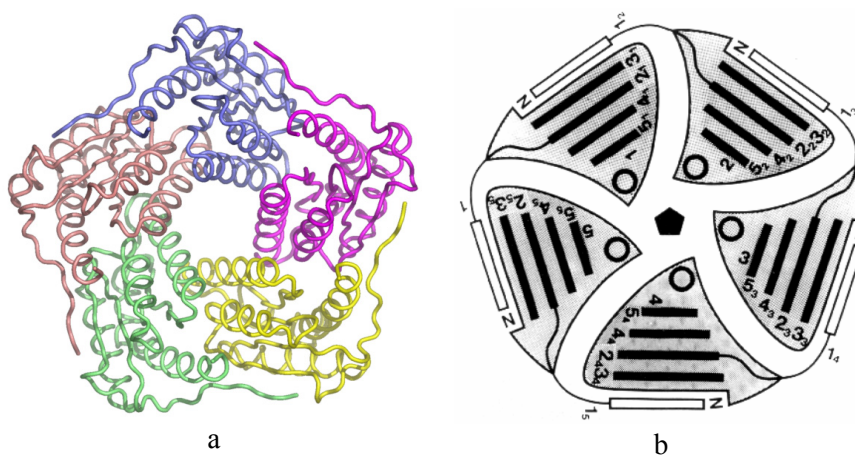


Fig 6. (a) C $\alpha$  model of a *B. subtilis* LS  $\beta$  subunit pentamer; (b) Schematical representation of  $\beta$  strands in a *B. subtilis* LS  $\beta$  subunit pentamer.

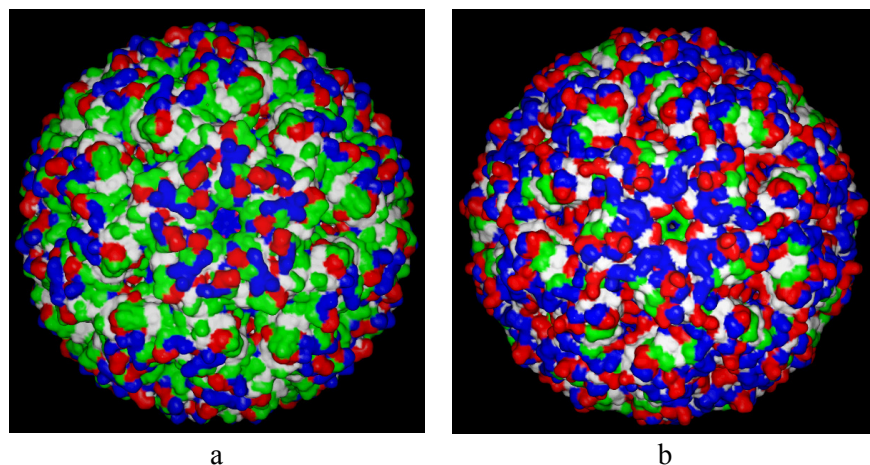


Fig 7. Surface representations of  $\beta_{60}$  capsids from (a) *B. subtilis* (b) *A. aeolicus* lumazine synthase. Color codes: red for Asp and Glu; blue for Lys, His and Arg; green for Asn, Gln, Ser, Thr, Cys, Tyr and Gly; white for Ala, Val, Leu, Ile, Met, Pro, Phe and Trp.

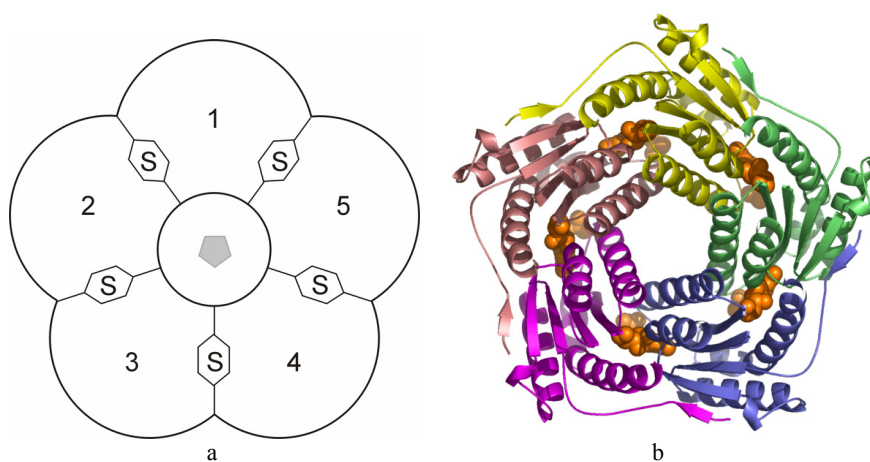


Fig 8. Ligand binding at the active sites in a  $\beta$  subunit pentamer from *B. subtilis* LS. (a) scheme; (b) structural representation.

A solvent accessible surface representation of entire  $\beta_{60}$  capsids from two LS homologs is shown in Fig 7. The capsid of *Bacillus subtilis* LS has a spherical shape and is characterized by a radially dipolar electrostatic

potential distribution with a positive electrostatic potential covering the inner capsid surface and a negative potential on the outer surface (Karshikoff & Ladenstein, 1989). Crystallographic binding studies of substrate analogous ligands have revealed the positions of the active sites at the subunit interfaces in a pentamer (Fig 8 a,b) close to the inner capsid surface (Ladenstein *et al.*, 1988). Ligand binding increases the stability of the capsid remarkably and drives the reassembly of  $\beta_{60}$  capsids from large  $T = 3$  capsids (see below).

#### 4. MODELLING OF THE BIFUNCTIONAL ENZYME COMPLEX

In spite of extensive crystallization screening and modification of the protein by mutation, we have never obtained diffraction quality crystals of *Bacillus subtilis* riboflavin synthase, the  $\alpha$  subunit trimers, which fill the core space of the icosahedral capsid.

A 2.0 Å resolution structure of *Escherichia coli* RS, obtained by multiple anomalous dispersion methods from the Se-Met derivative of the protein was described by Liao *et al* (2001). The homotrimer consisted of an asymmetric assembly of monomers, each of which comprised two structurally similar three-stranded  $\beta$  barrels with the same topology and a five-turn C-terminal  $\alpha$  helix. The similar  $\beta$  barrels, in fact N- and C-terminal domains, within the monomer confirm a prediction of pseudo-twofold symmetry inferred from the sequence similarity between the two halves of the monomer (Meining *et al.*, 1998; Schott *et al.*, 1990). The trimer interface comprised hydrophobic interactions from residues of the C-terminal  $\alpha$  helices of the three monomers. Only two of the three monomers were involved in a tightly associated inter-molecular surface between  $\beta$  barrels.

Consequently, the three active sites of the trimer were suggested to lie between pairs of monomers, where residues conserved among species reside. In the trimer, only one active site is formed and the other two active sites appear wide open and exposed to solvent. The nature of the trimer configuration as well as the imperfect local threefold symmetry suggested that only one active site could be formed at a time.

The structure of riboflavin synthase from *Schizosaccharomyces pombe* in complex with the substrate analog, 6-carboxyethyl-7-oxo-8-ribityllumazine has been determined at 2.1 Å resolution. In contrast to the homotrimeric solution state of native riboflavin synthase, the enzyme was found to be monomeric in the crystal structure. Structural comparison of the riboflavin synthases of *S. pombe* and *Escherichia coli* suggested oligomer contact sites and delineated the catalytic site for dimerization of the substrate and subsequent fragmentation of the pentacyclic intermediate. The pentacyclic substrate dimer was modeled into the proposed active site. It suggests that the substrate molecule at the C-terminal domain donates a four-carbon unit to the substrate molecule bound at the N-terminal domain of an adjacent subunit in the oligomer (Gerhardt *et al.*, 2002).

The catalytic formation of riboflavin molecules from lumazine precursors (Fig 1) in the core space of the capsid seems to occur under rather dynamic circumstances accompanied by large domain movements needed for the opening and closing of the active sites.

Fig 9 shows a computer model obtained by fitting the C<sub>α</sub> structure of *Escherichia coli* RS into the icosahedral LS capsid from *Bacillus subtilis* (Meining *et al.*, unpublished). The trimer axis of RS was aligned such that it is parallel with one of the icosahedral trimer axes. The RS trimer fits into the core space of the capsid remarkably well, however, large solvent-filled cavities can be recognized. It may be speculated that specific RS trimer conformations can be induced by interactions of RS with residues residing on the inner surface of the LS capsid as well as by interaction with the dimethyl-ribityl lumazine substrate (**3**, Fig 1). Association of RS and LS of *Bacillus subtilis* was reported to enhance catalytic efficiency through a substrate channeling mechanism (Kis *et al.*, 1995).

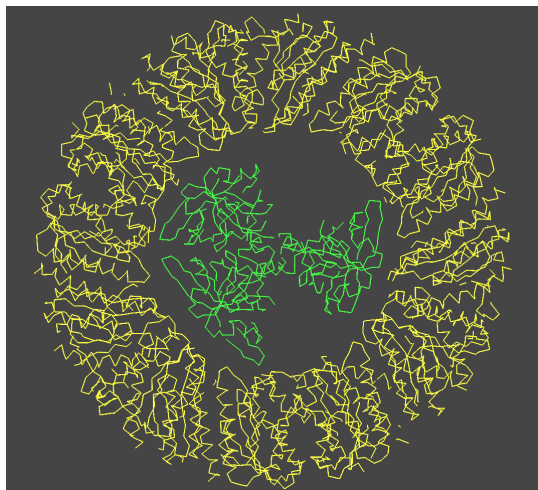


Fig 9. Computer-generated C $\alpha$  model of the LS/RS complex.

On a protomer basis, the  $k_{\text{cat}}$ (pH 7, 25°C) for *E. coli* RS is about tenfold that of *E. coli* LS (Zheng *et al.*, 2000). In this scenario the RS product (**1**) could bind to LS active sites and thus relieve product inhibition of RS (Kis, Volk *et al.*, 1995). There are six lumazine binding sites in a RS trimer. Interestingly, only two of them form a productive active site, while the other four binding sites only are capable of binding lumazine.

## 5. WHY ONLY PENTAMERS IN YEAST LUMAZINE SYNTHASE?

Several of the hitherto known lumazine synthases, among them LS from *Brucella abortus* (Goldbaum *et al.*, 1998), *Magnaporthe grisea* (Persson *et al.*, 1999), *Saccaromyces cerevisiae* (Meining *et al.*, 2000) and *Schizosaccharomyces pombe* (Fischer *et al.*, 2002, Gerhardt *et al.*, 2002) exist only as pentameric complexes. It was also shown that *Saccharomyces cerevisiae* LS did not associate with RS (Mörthl *et al.*, 1996). The question why only pentamers can be formed by yeast LS was intriguing, but could be solved by X-ray crystallography.

The structure in complex with a substrate analogous ligand (5-(6-D-ribylamino-2,4-dihydroxypyrimidine-5-yl)-1-pentyl-phosphonic acid) was solved at 1.85 Å resolution (see Fig 10a) by molecular replacement using the pentamer structure of the *Bacillus subtilis* LS capsid as a search model (Meining *et al.*, 2000).

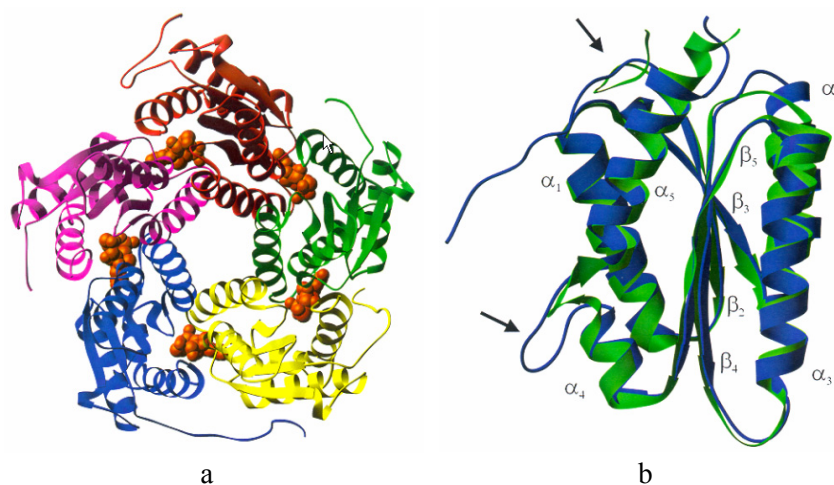


Fig 10. Model of a yeast lumazine synthase pentamer; (b) structural alignment of a yeast LS subunit (blue) and a *B. subtilis* LS subunit (green).

Structural determinants responsible for the inability of yeast LS to form an icosahedral capsid were detected by sequence alignment and structural alignment of the subunits of LS from *Saccharomyces cerevisiae* and *Bacillus subtilis* (Fig 10b): (1) an increase of the length of the loop in between helix  $\alpha_4$  and helix  $\alpha_5$  by four residues (sequence insertion: IDEA) and (2) differences in the conformations of the N-termini, which were completely flexible in LS from *Saccharomyces cerevisiae*. Up to four amino acid residues could be deleted from the N-terminus with not more than 40% loss of the enzymatic activity. The removal of 17 residues from the N-terminus resulted in still soluble protein with significantly reduced activity (5%), (Meining *et al.*, 2000). As reasons for the inability of certain lumazine synthases to form icosahedral assemblies, an insertion of two to four residues, which

extends the loop in between helix  $\alpha_4$  and helix  $\alpha_5$  and a proline residue in the N-terminus have been discussed.

If the yeast LS pentamers were assembled into an icosahedral structure by computer modeling, several clashes of certain main-chain parts and side-chains close to the trimer interfaces were visible (Fig 11).

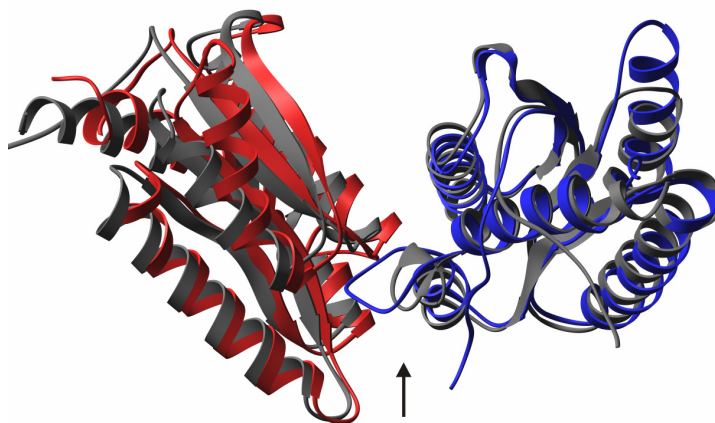


Fig 11. Computer-generated assembly of the yeast lumazine synthase pentamers in an icosahedral capsid.

In conclusion, it can be summarised, that capsid formation in icosahedral lumazine synthases may be perturbed by capping of the N-termini (impairment of the 5-stranded  $\beta$ -sheets in the pentamer), disorder in the conformation of the N-termini and by sequence insertions in the loop close to the trimer interface (clashes of main chain parts in icosahedral arrangement).

## 6. TOWARDS HIGH RESOLUTION AND EXTREME HEAT TOLERANCE – LS FROM AQUIFEX AEOLICUS

In the framework of our research on protein stability the X-ray structure analysis of LS from the hyperthermophilic bacterium *Aquifex aeolicus* was initiated in 1999. *Aquifex*, belonging to the genus *Thermotogales*, is

a marine hyperthermophile living close to volcanic hot water sources and grows optimally at  $T = 85\text{ }^{\circ}\text{C}$ . The structure analysis of this hyperthermostable form of LS revealed not only a surprising surface change of the icosahedral capsid, but opened up possibilities to study ligand binding and the structure of the active site at high resolution (1.6 Å). The moderate resolution of 3.3 Å obtained with LS from *Bacillus subtilis* did, in spite of well-defined averaged electron density maps, not allow crystallographic refinement and the analysis of the solvent structure and small side chain movements necessary to study the catalytic process in detail.

An open reading frame optimized for expression of LS from *Aquifex aeolicus* was expressed in *Escherichia coli* and the structure of the recombinant enzyme was solved by molecular replacement using LS from *Bacillus subtilis* as a search model. The structure was refined by maximum likelihood refinement (Murshudov *et al.*, 1997) to 1.6 Å resolution and  $R_{\text{free}} = 23.6\%$  (Zhang *et al.*, 2001). The subunit fold was closely related to that of *Bacillus subtilis* LS with an rmsd of  $C_{\alpha}$  carbons of 0.8 Å.

The icosahedral LS complex from *Aquifex aeolicus* showed an apparent melting temperature of 120 °C in a calorimetric scan and belongs therefore to the most thermotolerant known proteins. A comparison of the accessible surface comprised by charged residues with that of *Bacillus subtilis* LS revealed a doubling of charged residues on the surface of the *Aquifex* enzyme (See Fig 7) and the smallest fraction presented by energetically unfavourable hydrophobic surface residues. A relative increase in charged surface area and surface ionic networks is a characteristic determinant of proteins from hyperthermophiles and is related to their extreme heat tolerance. The strength of ionic interactions is due to solvation effects and the reduction of the dielectric constant of water increased at high temperature (Elcock, 1998; Karshikoff & Ladenstein, 2001). By formation of ionic networks the entropic penalty is reduced relative to pairwise interactions, an important contribution which increases the free stabilization energy of a protein according to the Gibbs-Helmholtz equation  $\Delta G_{\text{stab}} = \Delta H - T\Delta S$ .

## 7. NATURE IS NOT ALWAYS PREDICTABLE

The observation of the extended loop with the sequence insertion IDEA in between helix  $\alpha_4$  and helix  $\alpha_5$  in *Saccharomyces cerevisiae* LS has inspired us to test experimentally whether formation of an icosahedral capsid would be perturbed after the introduction of this insertion into the loop sequence of *Aquifex aeolicus* LS. We expected to observe an *Aquifex aeolicus* LS which could only form pentamers. Very surprisingly, however, the modified *Aquifex* LS formed large 48 S hollow sphere aggregates with a diameter of 300 Å (Fig 12a) indicating that the aggregation behavior of the subunits was indeed changed, but not in the direction we expected. Similar 48 S particles were observed earlier by pH-dependent disassembly of *Bacillus subtilis* LS capsids. The molecular weight determined from sedimentation data suggested particles with 180 subunits and T = 3 icosahedral symmetry.

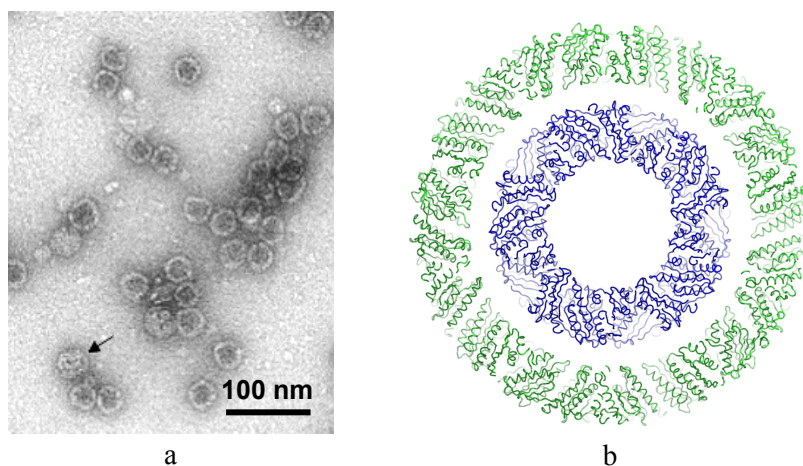


Fig 12. (a) 48S hollow capsids of *A. aeolicus* lumazine synthase with the sequence insertion IDEA; (b) size comparison of the models for small (26S) and large (48S) capsids.

By applying the concepts of quasi-equivalence implying that binding geometry and binding interactions are similar in pentamers and hexamers (Caspar & Klug, 1962), we have obtained a computer-generated model

of the presumptive  $T = 3$  capsid of *Aquifex* LS (Fig 12b, Zhang *et al.*, unpublished). This model, which represents the experimentally observed diameter of the large capsids surprisingly well, was obtained by extending the interactions in the hexamers and by decreasing the curvature of the capsid. This model, however, needs still to be verified either by cryo-electron microscopy in conjunction with image reconstruction or by X-ray crystallography. Preliminary results from cryo-electron microscopy suggest a diameter of 290 Å and a hexamer organisation, which is different from the hexamer structure obtained by simply extending the interfaces (Li *et al.*, unpublished). A careful inspection of the electron micrograph (Fig 12a) shows a number of filled particles (black arrow). The structural nature of these particles is unclear. The existence of double capsids, which are abundant in spherical viruses, is suggested, i.e. a  $T = 3$  capsid which contains a  $T = 1$  capsid in its core. The size comparison in Fig 12b shows that the diameters of both particles would be appropriate, at least.

## 8. LIGAND BINDING – A NUMBER OF UNSOLVED PROBLEMS

Early ligand binding studies by equilibrium dialysis have shown that a variety of 8-ribityl-substituted lumazines and 5-ribitylamino-pyrimidines, among them substrate **1** (see Fig 1), bind to *Bacillus subtilis* LS with a stoichiometry of one molecule per monomer corresponding to 60 molecules per capsid (Bacher & Mailander, 1978; Bacher & Ludwig, 1982). There is, however, also some binding affinity of the LS active site towards the product riboflavin (**4**, Fig 1) of the reaction catalyzed by RS. The enzyme from *S. pombe* was the first described lumazine synthase that was found to bind riboflavin with relatively high affinity ( $K_D$  of 1.2 mM) (Fischer *et al.*, 2002). The position and conformational orientation of bound riboflavin is similar to already known complex structures with substrate analogues. Comparing lumazine synthase crystal structures of either the isolated or the enzyme-inhibitor complexes from *B. subtilis* (Ladenstein *et al.*, 1994), *M. grisea*, spinach (Persson *et al.*, 1999) and *S. cerevisiae* (Meining *et al.*, 2000) with the crystal structure from *S. pombe*, clearly shows that riboflavin would act as a competitive inhibitor

( $K_i$  of 17  $\mu\text{M}$ , Fischer *et al.*, 2002) that binds in the same manner as the inhibitors of the other enzymes.

The icosahedral capsid has 60 identical binding sites for both substrates **2** and **3** (Fig 1). Each of these sites is located at the interface of two respective  $\beta$  subunits within a pentamer in close proximity to the inner capsid surface (Ladenstein *et al.*, 1988; 1994). The capsid structure with a thickness of the protein wall of 39  $\text{\AA}$  is rather densely packed, and the routes for the entry of the substrates and the exit of products are still unclear. Channels with a diameter of about 9  $\text{\AA}$  in *Bacillus subtilis* LS running along the 5-fold axes of the icosahedron (Fig 6a, above) would allow the passage of **1** and **2**, but appear too narrow for the exit of enzymatically produced riboflavin (**4**). An attempt to block the entrance of the five-fold channels by binding of five-fold symmetric tungsten compounds resulted in unperturbed enzymatic activity of the  $\alpha_3\beta_{60}$  complex from *Bacillus subtilis* (Ladenstein *et al.*, 1987).

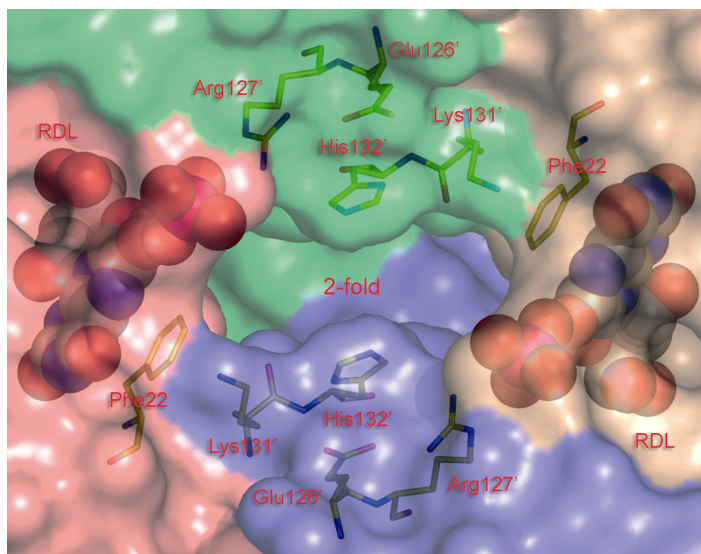


Fig 13. Pocket at the twofold local axes of *A. aeolicus* lumazine synthase.

Another route of substrate entry was suggested more recently: remarkably large pores were detected at the icosahedral twofold axes of *Aquifex aeolicus* LS (Zhang *et al.*, 2003), constituting the interfaces in

between pentamers (Fig 13). The pores at the twofold axes are formed by two symmetry equivalent tetrads of charged side-chains, comprising Arg127, His132, Glu126 and Lys131. The substrate binding sites were found close to the pore entrance. The pore appears large enough to allow diffusion of the substrate molecules **1** and **2** from solvent space to their binding sites. Single-site mutation studies have suggested that the catalytic activity of the enzyme is critically dependent on the presence of Arg127, which is a part of the charged tetrad, and on His88 as a proton donor/acceptor (Fischer *et al.*, 2003). In the substrate-free enzyme forms usually a bound phosphate ion is found involved in a charge-charge interaction with Arg127, which was thus defined as the phosphate binding site. Capsid stability is strongly influenced by pH, phosphate concentration and binding of substrate-analogous ligands (see following section). The question on how substrates, ligands and products penetrate the capsid wall might therefore be answered by assuming a substrate controlled capsid assembly/disassembly, which is coupled to the enzymatic function of the complex.

## **9. LIGAND BINDING, CAPSID STABILITY AND ASSEMBLY**

A number of experimental studies have shown that the stability of the T = 1 capsid is dependent on changes in pH, phosphate concentration and the presence of the substrates or certain substrate-analogous ligands (Fig 14, Bacher *et al.*, 1986). The electrostatic part of the subunit interaction energy has a pronounced minimum at  $\text{pH} \approx 8$  and is dependent on the presence or absence of substrate-analogous ligands. It was suggested that the pentamer is the most stable structure (- 4 kcal/mol pentamer at pH 8) among the three possible subunit assemblies and the trimer stability was characterized as repulsive with a negligible pH dependence (+ 2 kcal/mol trimer at pH 8). The electrostatic stabilities of pentamers and trimers appeared to be independent from the presence of the ligands, see Fig 15 (Karshikoff & Ladenstein, 1989).

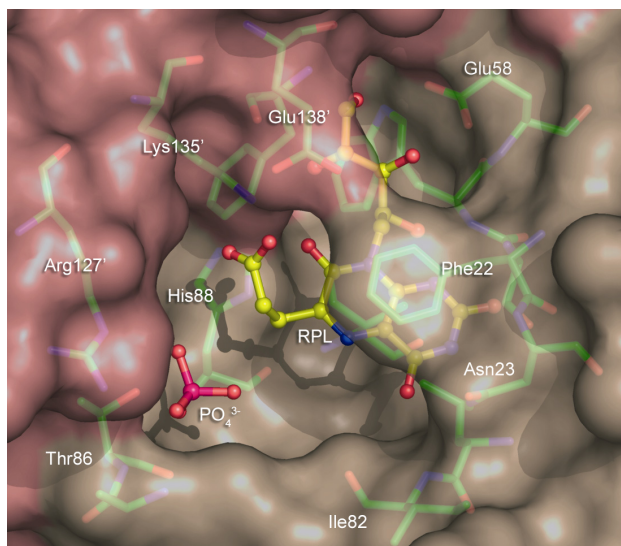


Fig 14. Substrate binding site of *A. aeolicus* lumazine synthase in complex with inhibitor 3-(7-hydroxy-8-ribityllumazine-6-yl)propionic acid.

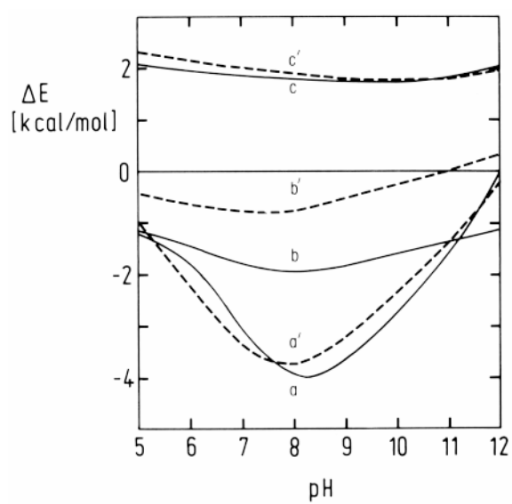


Fig 15. pH dependence of the electrostatic subunit interaction energy in  $\beta$  subunit – dimers, - trimers and – pentamers of *Bacillus subtilis* LS, a, pentamer, b, dimer, c, trimer, Curves a', b', c' correspond to the ligand-free forms, respectively.

The analysis has further shown that the aggregation/disaggregation equilibrium seems to be regulated by electrostatic interactions between  $\beta$  subunits forming dimers, which connect the relatively stable pentamers in the  $\beta_{60}$  capsid. The capsid may thus be considered as an assembly of 12 pentamers connected by the ligand-sensitive electrostatic dimer interactions. pH- or phosphate-dependent discharging of the tetrads at the twofold axes or the release of the ligand could lead to a weakening of the pentamer contacts via reduction of the electrostatic attraction within dimers, which is followed by dissociation of the entire capsid.

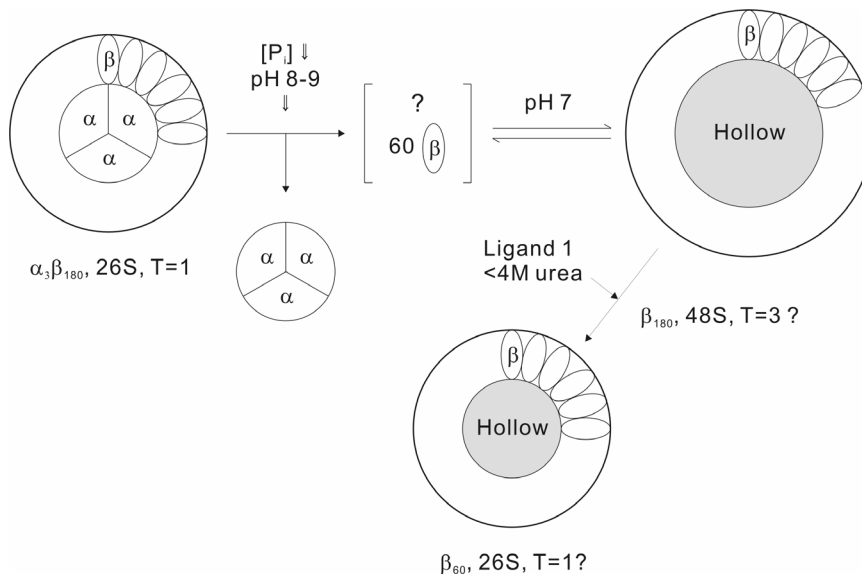


Fig 16. Disaggregation and ligand-driven reaggregation of *B. subtilis* LS capsids.

T = 1 capsids of *Bacillus subtilis* LS may be dissociated into  $\alpha$  subunit trimers and  $\beta$  subunits by treatment with buffers at pH > 8.5 and/or decrease of the phosphate concentration, schematically shown in Fig 16, which is supported by the experimental results from ultracentrifugation, X-ray scattering, electron microscopy and gel electrophoresis. Subsequent reduction of the pH led to the formation of large 48 S hollow sphere assemblies, which are best characterised by T = 3 icosahedral symmetry (see above). T = 3 assemblies, obtained in this way, can be

rearranged to form 26 S hollow  $T = 1$  particles in a ligand-driven reaction under the presence of urea. The binding of the ligand seems thus, in agreement with the electrostatic calculations, to add a favorable contribution to the subunit interaction energy and stabilize the  $T = 1$  capsid.

## 10. CATALYSIS AND ASSEMBLY

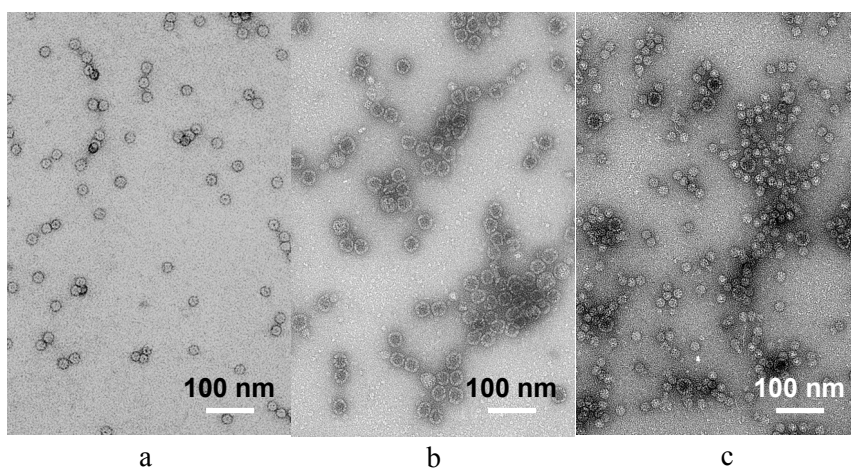


Fig 17. Negative staining electron micrographs of *B. subtilis* LS wild type (a), LS mutants R127T (b), R127H (c).

The only lethal single site mutation in the LS active site is the exchange of R127, the binding site for the phosphate group of the substrate **1**, to an uncharged residue, e.g. R127T. The mutants R127H and R127K still showed an enzymatic activity of 62% and 9% compared to the wildtype enzyme, respectively (Fischer *et al.*, 2003). R127 and R127' were identified as parts of the symmetry-related ionic tetrads at the local twofolds, comprising contacts in between pentamers (see above). It was found, that mutations at the phosphate binding site R127 are able to perturb enzymatic activity and, surprisingly enough, also capsid assembly. Electron micrographs obtained by negative staining and native acrylamide gel electrophoresis showed that the mutant protein R127H consisted of a mixture of  $T = 1$  and  $T = 3$  capsids, whereas in the mutant

proteins R127T and R127A almost exclusively large  $T = 3$  capsids were visible (Fig 17, Fischer *et al.*, unpublished). It is thus tempting to speculate that mutations of the residues comprising the ionic tetrads close to the icosahedral twofolds will show an impaired capsid assembly and possibly also changes in the enzymatic activity. It appears therefore, that enzymatic activity, capsid stability and assembly are coupled in the icosahedral lumazine synthase complex.

## References

1. Bacher, A., Baur, R., Eggers, U., Harders, H. D., Otto, M. K. & Schnepfle, H. Riboflavin synthases of *Bacillus subtilis*. Purification and properties. *J. Biol. Chem.* 1980; **255**: 632-637.
2. Bacher, A. & Ludwig, H. C. Ligand-binding studies on heavy riboflavin synthase of *Bacillus subtilis*. *Eur. J. Biochem.* 1982; **127**: 539-545.
3. Bacher, A., Ludwig, H. C., Schnepfle, H. & Ben-Shaul, Y. Heavy riboflavin synthase from *Bacillus subtilis*. Quaternary structure and reaggregation. *J. Mol. Biol.* 1986; **187**: 75-86.
4. Bacher, A. & Mailänder, B. Biosynthesis of riboflavin in *Bacillus subtilis*: function and genetic control of the riboflavin synthase complex. *J. Bact.* 1978; **134**: 476-482.
5. Bacher, A., Schnepfle, H., Mailänder, B., Otto, M. K. & Ben-Shaul, Y. (1980). *Flavins and Flavoproteins* (Yagi, K. Y., T., Ed.), Japan Scientific Societies Press, Tokyo.
6. Bricogne, G. Geometric sources of redundancy in intensity data and their use for phase determination. *Acta Cryst. Section A.* 1974; **30**: 395-405.
7. Bricogne, G. Methods and programs for direct-space exploitation of geometric redundancies. *Acta Cryst. Section A.* 1976; **32**: 832-847.
8. Caspar, D. L. D. & Klug, A. Physical principles in the construction of regular virus. *Cold Spring Harbor Symp. Quant. Biol.* 1962; **27**: 1-24.
9. Elcock, A. H. The stability of salt bridges at high temperatures: implications for hyperthermophilic proteins. *J. Mol. Biol.* 1998; **284**: 489-502.
10. Fischer, M., Haase, I., Kis, K., Meining, W., Ladenstein, R., Cushman, M., Schramek, N., Huber, R. & Bacher, A. Enzyme Catalysis via Control of Activation Entropy: Site-directed Mutagenesis of 6,7-Dimethyl-8-ribityllumazine Synthase. *J. Mol. Biol.* 2003; **326**: 783-793.

11. Fischer, M., Haase, I., Feicht, R., Gerhardt, S., Changeux, J. P., Huber, R. & Bacher, A. Biosynthesis of riboflavin. 6,7-Dimethyl-8-ribityllumazine synthase of *Schizosaccharo-mycetes pombe*. *Eur. J. Biochem.* 2002; **269**: 519-526
12. S. Gerhardt, I. Haase, J. Kaiser, R. Huber, A. Bacher und M. Fischer. Crystal structure of 6,7-dimethyl-8-ribityllumazine synthase of *Schizosaccharomyces pombe* in complex with riboflavin. *J. Mol. Biol.* 2002; **318**: 1317-1329
13. Goldbaum, F. A., Polikarpov, I., Cauerhff, A. A., Velikovskiy, C. A., Braden, B. C. & Poljak, R. J. Crystallization and preliminary x-ray diffraction analysis of the lumazine synthase from *Brucella abortus*. *J. Struct. Biol.* 1998; **123**: 175-178.
14. Harrison, S. C., Olson, A. J., Schutt, C. E., Winkler, F. K., Bricogne, G. Tomato bushy stunt virus at 2,9 Å resolution. *Nature.* 1978; **276**: 368-373.
15. Karshikoff, A. & Ladenstein, R. Electrostatic effects in a large enzyme complex: subunit interactions and electrostatic potential field of the icosahedral  $\beta_{60}$  capsid of heavy riboflavin synthase. *Proteins.* 1989; **5**: 248-257.
16. Karshikoff, A. & Ladenstein, R. Ion pairs and the thermotolerance of proteins from hyperthermophiles: a "traffic rule" for hot roads. *Trends Biochem. Sci.* 2001; **26**: 550-556.
17. Kis, K., Volk, R. & Bacher, A. Biosynthesis of riboflavin. Studies on the reaction mechanism of 6,7-dimethyl-8-ribityllumazine synthase. *Biochem.* 1995; **34**: 2883-2892.
18. Ladenstein, R., Bacher, A. & Huber, R. Some observations of a correlation between the symmetry of large heavy-atom complexes and their binding sites on proteins. *J. Mol. Biol.* 1987; **195**: 751-753.
19. Ladenstein, R., Ludwig, H. C. & Bacher, A. Crystallization and preliminary X-ray diffraction study of heavy riboflavin synthase from *Bacillus subtilis*. *J. Biol. Chem.* 1983; **258**: 11981-11983.
20. Ladenstein, R., Meyer, B., Huber, R., Labischinski, H., Bartels, K., Bartunik, H. D., Bachmann, L., Ludwig, H. C. & Bacher, A. Heavy riboflavin synthase from *Bacillus subtilis*. Particle dimensions, crystal packing and molecular symmetry. *J. Mol. Biol.* 1986; **187**: 87-100.
21. Ladenstein, R., Ritsert, K., Huber, R., Richter, G. & Bacher, A. The lumazine synthase/riboflavin synthase complex of *Bacillus subtilis*. X-ray structure analysis of hollow reconstituted  $\beta$ -subunit capsids. *Eur. J. Biochem.* 1994; **223**: 1007-1017.
22. Ladenstein, R., Schneider, M., Huber, R., Bartunik, H. D., Wilson, K., Schott, K. & Bacher, A. Heavy riboflavin synthase from *Bacillus subtilis*.

- Crystal structure analysis of the icosahedral  $\beta_{60}$  capsid at 3.3 Å resolution. *J. Mol. Biol.* 1988; **203**: 1045-1070.
23. Liao, D., Calabrese, J., Wawrzak, Z., Viitanen, P. & Jordan, D. Crystal structure of 3,4-dihydroxy-2-butanone 4-phosphate synthase of riboflavin biosynthesis. *Structure*. 2001; **9**: 11-18.
  24. Mailander, B. & Bacher, A. Biosynthesis of riboflavin. Structure of the purine precursor and origin of the ribityl side chain. *J Biol. Chem.* 1976; **251**: 3623-3628.
  25. Meining, W., Mörtl, S., Fischer, M., Cushman, M., Bacher, A. & Ladenstein, R. The atomic structure of pentameric Lumazine Synthase from *Saccharomyces cerevisiae* at 1.85 Å resolution reveals the binding mode of a phosphonate intermediate analogue. *J. Mol. Biol.* 2000; **299**: 181-197.
  26. Meining, W., Tibbelin, G., Ladenstein, R., Eberhardt, S., Fischer, M. & Bacher, A. Evidence for local 32 symmetry in homotrimeric riboflavin synthase of *Escherichia coli*. *J. Struct. Biol.* 1998; **121**: 53-60.
  27. Mörtl, S., Fischer, M., Richter, G., Tack, J., Weinkauff, S. & Bacher, A. Biosynthesis of riboflavin. Lumazine synthase of *Escherichia coli*. *J. Biol. Chem.* 1996; **271**: 33201-33207.
  28. Murshudov, G. N., Vagin, A. A. & Dodson, E. J. Refinement of Macromolecular Structures by the Maximum-Likelihood Method. *Acta Cryst. Section D*. 1997; **53**: 240-255.
  29. Nielsen, P., Neuberger, G., Floss, H. G. & Bacher, A. Biosynthesis of riboflavin. Enzymatic formation of the xylene moiety from [<sup>14</sup>C]ribulose 5-phosphate. *Biochemical & Biophysical Research Communications*. 1984; **118**: 814-820.
  30. Persson, K., Schneider, G., Jordan, D. B., Viitanen, P. V. & Sandalova, T. Crystal structure analysis of a pentameric fungal and an icosahedral plant lumazine synthase reveals the structural basis for differences in assembly. *Protein Science*. 1999; **8**: 2355-2365.
  31. Rossmann, M. & Blow, D. The detection of subunits within the crystallographic asymmetric unit. *Acta Cryst.* 1962; **15**: 24-31.
  32. Rossmann, M. G., Arnold, E., Erickson, J. W., Frankenberger, E. A., Griffith, J. P., Hecht, H. J., Johnson, J. E., Kamer, G., Luo, M., Mosser, A. G. & et al. Structure of a human common cold virus and functional relationship to other picornaviruses. *Nature*. 1985; **317**: 145-153.
  33. Van, Q. L., Keller, P. J., Bown, D. H., Floss, H. G. & Bacher, A. Biosynthesis of riboflavin in *Bacillus subtilis*: origin of the four-carbon moiety. *J. Bact.* 1985; **162**: 1280-1284.
  34. Weinkauff, S., Bacher, A., Baumeister, W., Ladenstein, R., Huber, R. & Bachmann, L. Correlation of metal decoration and topochemistry on protein surfaces. *J. Mol. Biol.* 1991; **221**: 637-645.

35. Zhang, X., Meining, W., Fischer, M., Bacher, A. & Ladenstein, R. X-ray Structure Analysis and Crystallographic Refinement of Lumazine Synthase from the Hyperthermophile *Aquifex aeolicus* at 1.6 Å Resolution: Determinants of Thermostability revealed from Structural Comparisons. *J. Mol. Biol.* 2001; **306**: 1099-1114.
36. Zhang, X., Meining, W., Cushman, M., Haase, I., Fischer, M., Bacher A., and Ladenstein R. A Structure-Based Model of the Reaction Catalyzed by Lumazine Synthase from *Aquifex aeolicus*. *J. Mol. Biol.* 2003; **328**: 167-182.
37. Zheng, Y.-J., Viitanen, P. V. & Jordan, D. B. Rate Limitations in the Lumazine Synthase Mechanism. *Bioorg. Chem.* 2000; **28**: 89-97.